Physica Medica 31 (2015) 929–933

Contents lists available at ScienceDirect

Physica Medica

journal homepage: http://www.physicamedica.com

Original Paper

Exposures in interventional radiology using Monte Carlo simulation coupled with virtual anthropomorphic phantoms

William S. Santos [a,*], Lucio P. Neves [b], Ana P. Perini [b], Walmir Belinato [c], Linda V.E. Caldas [a], Albérico B. Carvalho Jr. [c], Ana F. Maia [c]

[a] Instituto de Pesquisas Energéticas e Nucleares, Comissão Nacional de Energia Nuclear (IPEN-CNEN/SP), São Paulo, SP, Brazil
[b] Instituto de Física, Universidade Federal de Uberlândia (INFIS/UFU), Caixa Postal 593, 38400-902 Uberlândia, MG, Brazil
[c] Departamento de Física, Universidade Federal de Sergipe (UFS), São Cristovão, SE, Brazil

ARTICLE INFO

Article history:
Received 9 March 2015
Received in revised form 4 June 2015
Accepted 15 June 2015
Available online 6 July 2015

Keywords:
Interventional radiology
Computational dosimetry
Virtual anthropomorphic phantom

ABSTRACT

In this work we investigated the way in which conversion coefficients from air kerma-area product for effective doses (CC_E) and entrance skin doses (CC_{ESD}) in interventional radiology (IR) are affected by variations in the filtration, projection angle of the X-ray beam, lead curtain attached to the surgical table, and suspended shield lead glass in regular conditions of medical practice. Computer simulations were used to model an exposure scenario similar to a real IR room. The patient and the physician were represented by MASH virtual anthropomorphic phantoms, inserted in the MCNPX 2.7.0 radiation transport code. In all cases, the addition of copper filtration also increased the CC_E and CC_{ESD} values. The highest CC_E values were obtained for lateral, cranial and caudal projections. In these projections, the X-ray tube was located above the table, and more scattered radiation reached the middle and upper portions of the physician trunk, where most of the radiosensitive organs are located. Another important result of this study was to show that the physician's protection is 358% higher when the lead curtain and suspended shield lead glasses are used. The values of CC_E and CC_{ESD}, presented in this study, are an important resource for calculation of effective doses and entrance skin doses in clinical practice.

Introduction

Interventional radiology (IR) plays an important role in the diagnosis and treatment of vascular diseases, and other conditions that can lead to heart attacks and strokes. The technique uses fluoroscopy to guide the passage of a catheter into the region of the patient's heart. In general, the patient is examined for long periods of time during the procedure, and a large number of radiographic images are obtained [1,2]. To avoid the undesirable effects from ionizing radiation to the human health, it is necessary to maintain the radiation levels as low as reasonably achievable, taking into account economic and social factors [3].

The common principles of radiological protection, with respect to time, distance and shielding, are difficult to fully follow during IR procedures. This is mainly due to the complexity of the examinations, the necessary proximity of the physician to the patient and the need for a large set of images using different technical parameters, beam projection angles and additional protective equipment. Additionally, the elevated number of procedures performed contribute to increase the levels of radiation doses in medical professionals. To minimize the occupational dose absorbed by physicians, it is essential that they receive training in radiological protection, education about ionizing radiation sources and prior knowledge of the radiation levels they will be exposed to [4].

Considering the radiation exposure, it is impossible to directly determine the doses to the organs and tissues of the patient and physician. Therefore, computational exposure scenarios are necessary to determine conversion coefficients which allow the determination of organ doses, effective doses (E) or entrance skin doses (ESD) from a dosimetric quantity that can be easily obtained through experimental measurements, such as the air kerma-area product (KAP).

In recent years IR techniques have become quite common. The exposure of the personnel involved in IR procedures is relatively high, mainly due to their proximity to the irradiated part of the patient's body, and the time involved in these procedures. In the last years several studies have been presented about dose evaluation in patients and staff during IR procedures. Although several studies have been performed on occupational exposure IR with the Monte Carlo simulations [5,6], none of those calculated the dose conversion coefficients, in a realistic scenario of IR procedure, utilizing a *M*ale *A*dult me*SH* (MASH) virtual anthropomorphic phantom [7].

* Corresponding author. Tel.: +55 11 3133 9652; fax: +55 11 3133 9678.
E-mail addresses: wssantos@ipen.br (W.S. Santos), lucio.neves@ufu.br (L.P. Neves), anapaula.perini@ufu.br (A.P. Perini), wbfisica@gmail.com (W. Belinato), lcaldas@ipen.br (L.V.E. Caldas), ablohem@gmail.com (A.B. Carvalho), afmaia@ufs.br (A.F. Maia).

http://dx.doi.org/10.1016/j.ejmp.2015.06.011
1120-1797/

To calculate the conversion coefficients for E, some authors employed computational mathematical anthropomorphic phantoms (as in the work of Ferrari et al. [8]) while other authors have used voxel anthropomorphic phantoms [9]. In the latter study, the physician was represented by a voxel anthropomorphic phantom built in a lying position. In comparison with the anatomy of a standing person, this position causes the direction displacement of the internal organs. There may be also a sagittal diameter reduction, in particular at the abdominal region, which in turn can influence the estimated absorbed dose of organs and tissues. Thus, this type of phantom is not a realistic representation of an individual in a standing posture.

The anthropomorphic phantoms used in our study (MASH) were built on the basis of surface mesh and polygons, and were available in two postures, standing and lying. These are the most suitable faithful representations of the physician and the patient, and they have not previously been used in IR. Moreover, they were positioned in an IR room with the standard set of equipment that may influence the values of conversion coefficients by means of radiation scattering.

The virtual anthropomorphic MASH phantom was aimed to radiological protection studies, and therefore, it is necessary to maintain consistency in posture and anatomy. To maintain a realistic representation, the voxels of the matrices (that form the phantom) were resized to an edge of 0.24 cm long. This size is smaller than those from the literature, where normally larger voxel sizes are employed, which limits the precision on the contour of the organs. Consequently, with better organ definitions and contouring, results will be more accurate [7]. Furthermore, the results presented in the literature consider the physician as a "copy" of the patient. Therefore, the gravitational effects, which cause the overlap and displacement of the organs, were not evaluated. In this study, we employed phantoms in a lying and standing postures, aiming for a more realistic simulation.

We also used a detailed description of the components of a typical IR room, as well as the individual protection equipment, used by the staff and medical team. Within this, we could evaluate the efficiency of the lead curtain and suspended shield lead glass. These equipments are normally employed to protect the medical and staff from exposures from the primary and, mainly, the scattered radiation (from the operating table and the patient).

The mean absorbed doses to the tissues or organs may be low, but the concentrated dose depositions on a single spot may lead to a necroses of the organ or tissues. In the literature, there are several cases of skin injuries induced by the radiation on patients, from IR procedures [4].

Due to the high possibility of acute radiation symptoms for the skin, in this work, we presented the conversion coefficients (CC) results for the ESD as a function of the KAP, which take into account information regarding the place and field dimensions. These data allow the evaluation of the distribution of the absorbed dose in the irradiated skin of the patient.

The knowledge of the entrance skin doses may be used as a significant clinical information for the risk management to the patient and to the medical staff. The NCRP 168 [10] highlights the importance of the awareness regarding the high increase of medical exposition to ionizing radiation. In this sense, the doses received by the medical staff must be quantified. Therefore, one of the objectives of this work was to develop a methodology to determine the CCs for the skin. In the literature there are only a few papers that use Monte Carlo simulation to estimate this quantity, but they employed mathematical phantoms, or they did not consider the anatomical differences in position (laying and standing postures) [5,6,8,9,11–15]. Therefore, the methodology used in our work, and the results, provide a reliable estimative of the patient's entrance skin dose during an IR procedure, not addressed in previous papers.

In this study, a dosimetric evaluation using conversion coefficients calculated for a patient and a physician under different technical parameters and image acquisition conditions used in an angiographic system was carried out. In this work, a much more realistic representation was performed, utilizing a realistic IR room and a MASH virtual anthropomorphic phantom, for both patient and physician. Besides that, parameters not considered in previous studies were considered, such as the lead curtain and suspended shield lead glass. Although most information is specific to procedures performed in an angiographic system, some aspects of the results are relevant for all IR procedures.

Materials and methods

In IR procedures, the main focus for radiological risk is the patient who is exposed to the primary beam, and the physician who is mainly exposed to the photons scattered by the patient, the operating table and the image intensifier [16]. Therefore, estimating the radiation doses for both patient and physician requires the use of two computational anthropomorphic phantoms: a model to represent the patient lying on the surgical table and another to represent the physician, in a standing position.

In this study, two irradiation scenarios were modelled: in the first one, the lead curtain attached to the surgical table and shield suspended lead glass were not available, while in the second one, the use of these protective equipment was considered. The complete computational scenario was elaborated, and two anthropomorphic phantoms, IR equipment, and a room with real dimensions and real material walls were included, as can be seen in Fig. 1.

Seven types of beam projection angles were studied: left anterior oblique, 45° (LAO45), posterior anterior (PA), right anterior oblique, 45° (RAO45), caudal, 30° (CAUD30), left lateral, 90° (LAO90), right lateral, 90° (RAO90) and cranial, 30° (CRAN30) to focal surface distances (FSD) of 56.6, 50, 40, 43.6, 40, 40 and 45 cm, respectively. The physician was positioned 17 cm from the left side at the waist level of the patient.

To represent the patient and the physician, a modified MASH adult anthropomorphic phantom [17] was used in each case. This phantom was developed by the Computational Dosimetry Group/Federal University of Pernambuco (Brazil). It was based on anatomical and physiological data of a reference male from ICRP 89 [18]. It presents more than 100 organs and tissues that are relevant for dosimetry. The main physiological data of the adult anthropomorphic phantom were height of 175.6 cm and body mass of 72.7 kg. To avoid computational memory problems, the original phantom matrices were resized for a voxel edge of 0.24 cm. It is important to note that as in any simulation, some limitations may be observed. Given the static nature of the simulations, the variation in size of some organs, due to the movement of the patient or the blood flow, were not considered in this work.

We used the MCNPX 2.7.0 [19] radiation transport code. This code can handle the transport and interaction of neutrons, photons and electrons in a wide range of energies and for arbitrary three-dimensional geometries. The technical parameters used in the computational simulation were obtained from the literature: peak voltage of 80 kVp, anode angle of 12°, tungsten target material, and a three filter set of 3.5 mmAl, 3.5 mmAl + 0.2 mmCu and 3.5 mmAl + 0.5 mmCu.

The spectra were generated using a software from Report 78 [20]. An ionization chamber, placed on the output of the X-ray tube, was modelled as an air object with a volume of $10 \times 10 \times 1$ cm^3. The absorbed dose in the volume of air in the ionization chamber was recorded using the MCNPX tally *F6* (in MeV/g) and then converted to the unit of J/kg, or Gy.

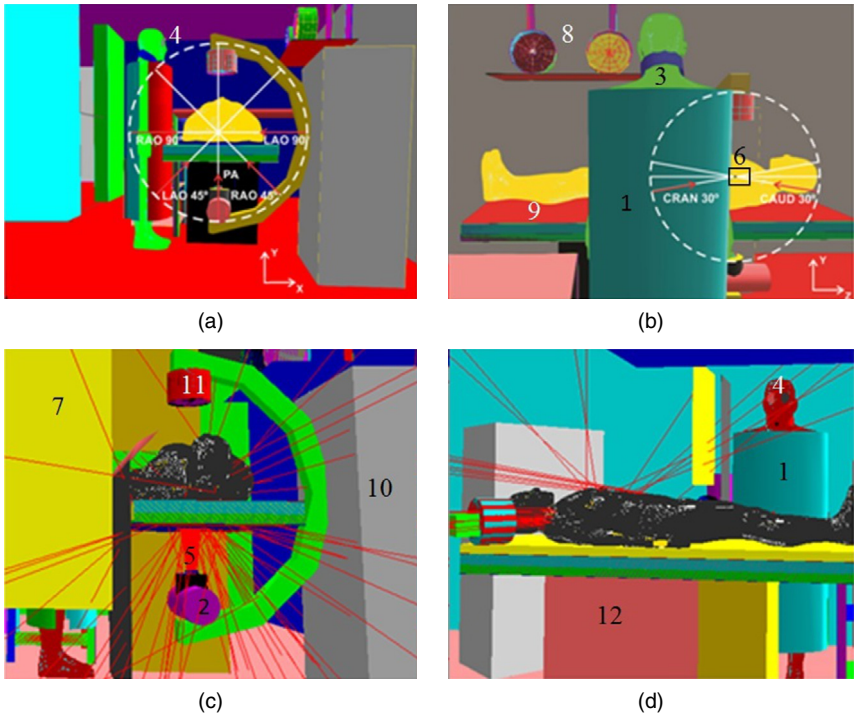

Figure 1. In (a) and (b) first scenario in different views and in (c) and (d) second scenario in different views, showing the main components of a room of interventional procedures of the irradiation scenarios: (1) lead apron; (2) X-ray tube; (3) thyroid shield; (4) lead glasses; (5) KAP measure system; (6) ESD measurement system; (7) suspended shield lead glass; (8) video monitors; (9) surgical table; (10) X-ray equipment; (11) image intensifier and (12) lead curtain attached to the surgical table.

Lead aprons, thyroid shields and glasses of 0.5 mmPb were added to the physician. The surgical table was modelled with dimensions of $185 \times 66 \times 9.25$ cm^3 (length × width × thickness) and with real chemical and physical characteristics, using foam, carbon fibre and metal alloy on its support base.

The KAP, the most common risk quantity in IR procedures, per procedure, was determined by multiplying the dose in the ionization chamber by the beam area. The absorbed dose in every major organ of the MASH anthropomorphic phantom was determined using the MCNPX tally energy deposition **F8* (in MeV). This tally records the energy deposited in the region of interest by all the primary and secondary particles, and was subsequently converted to conversion coefficients for equivalent dose. With the knowledge of these values in each organ and tissue, it was possible to calculate the conversion coefficients for E based on the tissue weighting factors, w_T, of ICRP 120 recommendations [4]. As this quantity cannot be measured directly, it is common to use computational exposure models for the determination of conversion coefficients, which allows the determination of E from a measurable quantity.

To obtain the patient's ESD, a second ionization chamber was inserted in the simulation. This ionization chamber had dimensions of $10 \times 10 \times 1$ cm^3 and was filled with atmospheric air. In all projections, it was positioned near the skin of the patient, and perpendicular to the radiation beam. The results were scored as MeV/g, employing the *tally F6*. The results of this study are presented in terms of conversion coefficients of KAP to E and ESD. These conversion coefficients of KAP to E, given by E/KAP and to ESD, given by ESD/KAP, will be referred as CC_E and CC_{ESD} throughout this work.

In all the simulations, 10^9 histories were performed to ensure that the statistical errors were acceptable. The typical CPU time varied between 24 and 63 h, on a PC with an i7 core processor and 16 Gb of RAM, depending on the bem filtration and projection. The statistical uncertainties (type A) were calculated using the statistical errors of the deposited energy of organs and tissues and in the air volume of the ionization chamber, all provided by the MCNPX code.

Results and discussion

In this study, CC_E and CC_{ESD} values for various types of projection angles used in angiography procedures were obtained. This procedure was undertaken for the three studied tube filtration sets: 3.5 mmAl, 3.5 mmAl + 0.2 mmCu and 3.5 mmAl + 0.5 mmCu and, furthermore, the effect of using lead curtain and the suspended protectors on the CC_E and CC_{ESD} were evaluated. Two adult phantoms were used to represent a male physician and a patient, and the conversion coefficients were calculated for seven beam projection angles centred at the patient's heart.

Conversion coefficients of air kerma-area product for effective dose to the physician

Table 1 shows the CC_E obtained for the physician. The results clearly show the importance of the lead curtain and suspended shield lead glass. These protective devices, with an equivalent lead thickness of 0.5 mm, reduced the CC_E in 71%, 358% and 300%, for the filters of 3.5 mmAl, 3.5 mmAl + 0.2 mmCu and 3.5 mmAl + 0.5 mmCu, respectively.

Bozkurt and Bor [9] and Siiskonen et al. [5] determined the CC_E to the physician during a cardiac interventionist procedure. In these studies, a 3.5 mmAl filter, 80 kVp tube voltage and 10×10 cm^2 filed size were employed. The values obtained were 0.145 μSv/Gy.cm^2 and 0.04 μSv/Gy.cm^2, respectively.

In these studies, the physician was represented, respectively, by an anthropomorphic tomographic phantom and a mathematic phantom. These phantoms were all in laying positions. As listed in Table 1, the values presented in our study, for 3.5 mmAl, are lower than those presented in the literature. These differences are associated to the anatomical deformations, caused by the gravitational force, as the displacement of internal organs of the thorax, lungs compression, reduction of the sagittal diameter, changes in the

Table 1
CC_E for the physician as a function of beam filtration and projection. The statistical uncertainties, in %, are given in parentheses.

Projection	CC_E (μSv/Gy cm^2)					
	Without lead curtain and suspended lead glass			With lead curtain and suspended lead glass		
	3.5 mmAl	3.5 mmAl + 0.2 mmCu	3.5 mmAl + 0.5 mmCu	3.5 mmAl	3.5 mmAl + 0.2 mmCu	3.5 mmAl + 0.5 mmCu
PA	5.3E-02 (1.5)	9.3E-02 (1.9)	1.3E-01 (2.1)	5.1E-03 (2.7)	1.0E-02 (2.1)	1.9E-02 (2.1)
LAO90°	5.6E-02 (1.4)	1.1E-01 (1.4)	1.4E-01 (1.5)	3.7E-02 (1.3)	5.6E-02 (1.1)	8.2E-02 (2.2)
RAO90°	1.1E-02 (1.5)	1.9E-01 (2.5)	2.6E-01 (3.0)	5.8E-03 (1.6)	1.0E-01 (2.6)	1.7E-01 (2.3)
CRAN30°	9.4E-02 (1.1)	1.6E-01 (1.5)	2.1E-01 (0.6)	1.6E-02 (1.5)	2.4E-02 (1.5)	3.5E-02 (1.1)
CAUD30°	1.0E-02 (1.5)	1.9E-01 (1.1)	2.6E-01 (2.8)	3.0E-02 (1.8)	5.7E-02 (1.1)	1.0E-01 (2.2)
RAO45°	2.4E-02 (1.6)	4.3E-02 (1.3)	5.8E-02 (1.6)	8.8E-03 (1.7)	1.3E-02 (1.4)	1.8E-02 (1.1)
LAO45°	2.3E-02 (1.3)	4.2E-02 (1.0)	5.7E-02 (1.3)	5.2E-03 (1.5)	7.4E-03 (1.2)	1.0E-02 (0.0)
Average	2.4E-02 (1.5)	1.1E-01 (1.4)	1.4E-01 (1.6)	1.4E-02 (1.6)	2.4E-02 (1.4)	3.5E-02 (2.1)

position of the arms and shoulders, and cranial displacement. These aspects were considered in this study, but not in previous ones.

According to Cassola et al. [7], the differences between the absorbed doses on the organs and tissues, when comparing the results using the anthropomorphic phantoms on the sitting and supine positions may be up to 60%. Besides that, in our work, several typical IR equipment were introduced in the simulation scenario. These equipment, and the anatomical and morphological differences between the phantoms, justify these differences.

Conversion coefficients of air kerma-area product for effective dose and entrance skin dose to the patient

As it is impracticable, or clinically impossible, to measure the absorbed doses in vivo, in this study the patient's CC_E were calculated. These values are useful to evaluate the potential risk of stochastic effects, as cancer. Besides stochastic effects, it is well known that the concentrated radiation deposition may cause tissue necrosis (a deterministic effect). Examples are the radiation induced lesions on the patient's skin during IR procedures [4]. When the fluoroscopy time is long, or when the radiation beam is used in only one projection, there is an increase in the risk for skin injuries. Therefore, in this study we also present the CC_{ESD} results, taking into consideration information regarding the position and dimensions of the radiation field. These information allow the evaluation of the absorbed dose distribution on the patient's skin. The CC_{ESD} and CC_E values as a function of beam filtration and projections for the patient are listed in Table 2.

The mean value of the CC_E for the patient, during a complete procedure, presented in Table 2, shows good agreement with some values in the literature 1.40E-01 mSv/Gy cm^2 [21], 1.85E-01 mSv/Gy cm^2 [22] and 1.20E-01 mSv/Gy cm^2 [23] (range 0.100–0.280). These values were determined experimentally. The addition of copper filtration is used to reduce the KAP to the patient, as well as E and the ESD, but the KAP reduction is much more pronounced. Therefore, the values of CC_E and CC_{ESD} increase with the addition of filtration.

In the absence of a direct measurement, the CC_{ESD} presented in this work may be applied to determine the ESD in cardiac coronary angiography procedures. These data present a good agreement with some results published in the literature: 3.8 mGy/Gy cm^2[24], 3.9 Gy/Gy cm^2[25] and 4.3 mGy/Gy cm^2[26]. Therefore, as the ESD monitoring in real time is very difficult, it is impossible to foresee the maximum exposure location before the procedure.

The X-ray tube orientation has a strong influence on the CC_E variations. When the X-ray tube is in the undercouch position, i.e., PA, RAO45° and LAO45° projections, the patient CC_E decrease compared to those with the overcouch tube position. In these projections, the spine of the patient and surgical table result in a beam filtration of low energy photons that contribute to decrease the intensity of the transmitted radiation, and consequently, lower values of energy are absorbed by organs located in the thoracic region of the patient. The overcouch X-ray tube positions (CRAN30° and CAUD30°) and right lateral (RAO90°) caused the highest CC_E. Due to a strong radiation scattering from the patient, the CAUD30 projection was considered the most critical. In these projections, more scattered radiation reaches the middle and upper portions of the trunk, where most of the radiosensitive organs are located closer to the entrance surface.

For all projection angles, the results showed that the CC_E received by the patient and physician increase with increasing copper filtration. The beam hardening, as a consequence of the additional copper filtration, leads to a higher mean CC_E. These values increase with the addition of the 0.2 mmCu and 0.5 mmCu filtration by 56% and 81% for the patient, 358% and 483% for the physician, without the use of lead curtain and suspended shield, and 71% and 150% for the physician when the lead curtain and suspended shield were available.

In all cases the CC_E are also higher for incident angles oriented from the right side than for those from the left side. This asymmetry occurs because the specification of the CC_E includes several unpaired organs oriented towards one side of the body. Also, in these projection angles, the physician is closer to the X-ray tube and therefore he is submitted to a very high scattered radiation beam.

Table 2
CC_E and CC_{ESD} for the patient as a function of beam filtration and projection. The statistical uncertainties, in %, are given in parentheses.

Projection	CC_E (mSv/Gy.cm^2)			CC_{ESD} (mGy/Gy.cm^2)		
	3.5 mmAl	3.5 mmAl + 0.2 mmCu	3.5 mmAl + 0.5 mmCu	3.5 mmAl	3.5 mmAl + 0.2 mmCu	3.5 mmAl + 0.5 mmCu
PA	4.3E-02 (0.6)	1.0E-01 (0.1)	1.3E-01 (0.1)	2.7 (4.1)	3.6 (6.5)	4.1 (7.4)
LAO90°	1.6E-01 (0.5)	2.5E-01 (0.2)	2.9E-01 (0.2)	6.4 (3.3)	6.5 (8.8)	6.5 (9.4)
RAO90°	1.8E-01 (0.1)	2.9E-01 (0.2)	3.4E-01 (0.2)	6.4 (4.3)	6.5 (8.7)	6.5 (9.4)
CRAN30°	2.2E-01 (0.2)	3.4E-01 (0.1)	4.1E-01 (0.1)	6.4 (5.3)	6.4 (8.7)	6.4 (9.3)
CAUD30°	1.7E-01 (0.2)	2.8E-01 (0.2)	3.3E-01 (0.2)	6.9 (5.5)	6.9 (9.4)	6.9 (10)
RAO45°	1.3E-02 (0.5)	3.1E-02 (0.1)	4.1E-02 (0.1)	1.4 (3.1)	1.6 (4.4)	1.7 (4.7)
LAO45°	1.5E-02 (0.3)	3.4E-02 (0.1)	4.4E-02 (0.1)	1.7 (3.2)	1.9 (4.8)	2.0 (5.0)
Average	1.6E-01 (0.3)	2.5E-01 (0.1)	2.9E-01 (0.1)	4.6 (4.1)	4.8 (8.5)	4.9 (7.9)

It is important to note that, in clinical practice, the voltage (kV) of the X-ray tube varies with the thickness of the examined region of the patient. For patients with a thicker layer of adipose tissue, the automatic exposure control (AEC) of X-ray equipment increases in voltage in order to compensate for the increase of beam attenuation by the patient's body, and then producing a clinically useful image. For a slim patient, the voltage decreases. In this sense, variations of CCs in IR procedures are expected, because the patient's anthropomorphic characteristics may vary. Thus the CC_E presented in this study are valid for patients with physiological characteristics close to the anthropomorphic phantom, for which the values were calculated. In the case of the MASH phantom, its features correspond to those of a man with an average height and weight, which is the standard subject from ICRP 89 [18].

Conclusions

The CC_E and CC_{ESD} values for the physician and the patient at IR cardiac procedures were evaluated for seven beam projections, and three types of beam filtration. In addition, we evaluated the influence of the lead curtain attached to the surgical table, and suspended lead glass shield, in reducing CC_E for the physician. As shown in this study, the use of such protective devices may reduce the physician CC_E up to 358%.

The highest CC_E values were obtained for lateral (LAO90° and RAO90°), cranial (CRAN30°) and caudal (CAUD30°) projections. In these projections, the X-ray tube is located above the table, which justifies higher CC_E for the patient. In these cases, more scattered radiation reaches the middle and upper portions of the physician's trunk where most of the radiosensitive organs are located, closer to the entrance surface. Furthermore, the increase of the copper filtration was followed with an increase of the CC_E and CC_{ESD} values.

Acknowledgement

The authors of this paper received support from the Brazilian agencies: CAPES (Project Pró-Estratégia no. 1999/2012) CNPq (Grant no. 304789/2011-9) and INCT–Project INCT for Radiation Metrology in Medicine (Grant no. 573659/2008-7).

References

[1] Topaltzikis T, Rountas C, Moisidou R, Fezoulidis I, Kappas C, Theodorou K. Radiation dose to patients and staff during angiography of the lower limbs. Derivation of local dose reference levels. Phys Med 2009;25(1):25–30.
[2] Morrish OWE, Goldstone KE. An investigation into patient and staff doses from X-ray angiography during coronary interventional procedures. Br J Radiol 2008;81(961):35–45.
[3] ICRP 103. Valentin DJ editor.. The 2007 Recommendations of the International Commission on Radiological Protection (ICRP) Publication 103 Ann. ICRP; 2007.
[4] ICRP 120. vol. 42. Radiological protection in cardiology. Commission on Radiological Protection (ICRP) Publication 120 Ann. ICRP; 2013. p. 69–79.
[5] Siiskonen T, Tapiovaara M, Kosunen A, Lehtinen M, Vartiainen E. Monte Carlo simulations of occupational radiation doses in interventional radiology. Br J Radiol 2007;80(954):460–8.
[6] Koukoravaa C, Carinou E, Ferrari P, Krim S, Struelens L. Study of the parameters affecting operator doses in interventional radiology using Monte Carlo simulations. Radiat Meas 2011;46(11):1216–22.
[7] Cassola VF, Kramer R, Khoury HJ. Posture-specific phantoms representing female and male adults in Monte Carlo-based simulations for radiological protection. Phys Med Biol 2010;55(15):4399–430.
[8] Ferrari P, Venturi G, Gualdrini G, Rossi PL, Marriseli M, Zannoli R. Evaluation of the dose to the patient and medical staff in interventional cardiology employing computational models. Radiat Prot Dosim 2010;141(1):82–5.
[9] Bozkurt A, Bor D. Simultaneous determination of equivalent dose to organs and tissues of the patient and of the physician in interventional radiology using the Monte Carlo method. Phys Med Biol 2007;52(2):317–30.
[10] NCRP. Radiation dose management of fluoroscopically-guided interventional medical procedures, National Council on Radiation Protection and Management. Report 168, Maryland: Bethesda; 2011.
[11] Santos WS, Carvalho JRAB, Hunt JG, Maia AF. Using the Monte Carlo technique to calculate dose conversion coefficients for medical professionals in interventional radiology. Radiat Phys Chem 2014;95:177–80.
[12] Balter SS, Hopewell JW, Miller DL, Wagner LK, Zelefsky MJ. Fluoroscopically guided interventional procedures: a review of radiation effects on patients' skin and hair. Radiology 2010;254:326341.
[13] Lee C, Lee C, Bolch W. Age-dependent organ and effective dose coefficients for external photons: a comparison of stylized and voxel-based pediatric phantoms. Phys Med Biol 2006;51:46634688.
[14] Schlattl H, Zankl M, Petoussi-Henss N. Organ dose conversion coefficients for voxel models of the reference male and female from idealized photon exposures. Phys Med Biol 2007;52:21232145.
[15] Park SH, Lee JK, Lee C. Dose conversion coefficients calculated using tomographic phantom, KTMAN-2, for X-ray examination of cardiac catheterisation. Radiat Prot Dosim 2008;128:351358.
[16] Beth AS, Thomas JV, Haraldur B, Anthony WS. An investigation of operator exposure in interventional radiology. Radiographics 2006;26(5):1533–9.
[17] Cassola VF, de Melo Lima VJ, Kramer R, Khoury HJ. FASH and MASH: female and male adult human phantoms based on polygon meSH surfaces. Part I: development of the anatomy. Phys Med Biol 2010;55(1):133–62.
[18] ICRP 89. Basic anatomical and physiological data for use in radiological protection: reference values. Oxford: International Commission on Radiological Protection (ICRP) Publication 89 Pergamon Press; 2003.
[19] Pelowitz DB. MCNPX user's manual, version 2.7.0. Report LA-CP-11–00438, Los Alamos National Laboratory; 2011.
[20] Cranley K, Gilmore BJ, Fogarty GWA, Desponds L. Catalogue of diagnostic x-ray spectra and other data. Institute of Physics and Engineering in Medicine; 1997, Report 78 York: IPEM.
[21] Samar ET, Aroua A, Bochud FO, Delabays A, Laedermann JP, Verdum FR. Patient radiation risk in interventional cardiology. OMICS J Radiol 2012;1(2), 103 1–9.
[22] Bogaert E, Bacher K, Thierens H. A large-scale multicentre study in Belgium of dose area product values and effective doses in interventional cardiology using contemporary X-ray equipment. Radiat Prot Dosim 2008;128(3):312–23.
[23] NCRP. Ionizing radiation exposure of the population on the United States National Council on Radiation Protection and Measurements. Report 160 Bethesda, 2009.
[24] Chida K, Saito H, Otani H, Kohzuki M, Takahashi S, Yamada S, et al. Relationship between fluoroscopic time, dose-area product, body weight, and maximum radiation skin dose in cardiac interventional procedures. AJR Am J Roentgenol 2006;186(3):774–8.
[25] Karambatsakidou A, Tornvall P, Saleh N, Chouliaras T, Lofber PO, Fransson A. Skin dose alarm levels in cardiac angiography procedures: is a single DAP value sufficient? Br J Radiol 2005;78(933):803–9.
[26] Quai E, Padovani R, Peterzol A, Vano E, Guibelalde E, Toivonen M. Maximum skin dose assessment in interventional cardiology: results in three different European hospitals. Eur Radiol 2003;13:542.